Morphology and Mechanical Properties of Blends of Isotactic or Syndiotactic Polypropylene with SEBS Block Copolymers

STEFAN SETZ, FLORIAN STRICKER, JÖRG KRESSLER,* THOMAS DUSCHEK, and ROLF MÜLHAUPT

Albert-Ludwigs-Universität Freiburg, Institut für Makromolekulare Chemie und Freiburger Materialforschungszentrum, Stefan-Meier-Straße 31, D-79104 Freiburg i. Br., Germany

SYNOPSIS

Blends of poly(styrene)-*block*-poly(ethene-*co*-but-1-ene)-*block*-poly(styrene) (SEBS) with isotactic polypropylene (PP) and syndiotactic PP, respectively, were investigated. The morphology was observed by means of scanning electron microscopy (SEM) and transmission electron microscopy (TEM). The cryofracture surfaces studied by SEM did not show any particles that were pulled out, so that a good compatibility between SEBS and different PPs could be assumed. The multiphase character of the blends could be well detected by TEM of RuO_4 stained samples. TEM micrographs of two-layer specimens revealed that SEBS tends to diffuse into the PP phase under formation of micelles. The block copolymer shows a reorientation phenomenon of large domains at the interface before the diffusion into the PP phase occurs. The interfacial strength as a function of annealing time was measured by a peel test of two-layer specimens. Mechanical properties are studied and related to the blend morphology. © 1996 John Wiley & Sons, Inc.

INTRODUCTION

Poly(styrene)-*block*-poly(ethene-*co*-but-1-ene)-*block*-poly(styrene) (SEBS) is frequently used as toughening agent for brittle polymers. SEBS is a microphase separated thermoplastic elastomer where the polystyrene (PS) blocks at both ends are associated in rigid domains that form a lattice in the flexible poly(ethene-*co*-but-1-ene) (EB) matrix.[1] Usually SEBS contains less than 35 wt % PS. Interfacial tension and interfacial adhesion plays an essential role when SEBS is used as a compatibilizing and toughening agent, because the improvement of impact properties is frequently achieved by energy dissipation at interfaces of immiscible blends and composites.[2] Generally speaking, a block copolymer should lower the interfacial tension in order to achieve a well-dispersed phase morphology[3,4]; and additionally it should increase the interfacial adhesion, which is mainly determined by the number of bonds crossing from one phase into another.[5] Thus if the block copolymer molecular weight is high enough, it can act at both sides of the interface as an anchor. Therefore, SEBS is usually used in blends where one component shows a good compatibility with the olefinic block and the other component has a good compatibility with the styrene blocks. Here the term compatibility means that sufficient mechanical properties can be achieved. This does not mean miscibility in a thermodynamic sense. Blends of polypropylene (PP) with polycarbonate,[6,7] acrylonitrile–butadiene–styrene (ABS),[8] high-density polyethylene (HDPE),[9,10] or linear low-density PE (LLDPE)[10] were compatibilized with SEBS. Especially maleinated SEBS (SEBS-*g*-MA) is used for reactive blending, for example, in combination with PP for ternary blends containing also polyamides.[11,12] In these blends best results were achieved when a mixture of SEBS and SEBS-*g*-MA was used.[13] Here it is assumed that the EB block has a good compatibility with PP and the interfacial adhesion between polyamide and SEBS is improved by the imide formation during the reaction of amine end groups with succinic anhydride. It was also pos-

* To whom correspondence should be addressed.

Journal of Applied Polymer Science, Vol. 59, 1117–1128 (1996)
 CCC 0021-8995/96/071117-12

Table I Characterization of Polymers Used

Polymer	Source	M_n[a] (g/mol)	M_w/M_n	mmmm[b] (%)	rrrr[b] (%)	T_g[c] (°C)	T_m[d] (°C)	T_{cryst}[d] (°C)
i-PP108k	Lab.[e]	108,000	2.3	96.6	—	4	153.8	104.0
s-PP104k	Lab.[e]	104,000	1.7	—	90.4	10	148.2	85.4
i-PP183k	BASF	183,000	2.0	94	—	3	148.0	95.1
s-PP106k	Mitsui Toatsu	106,000	1.7	0.4	68.6	9	124	60.5
*i*PP46k[f]	Shell	46,500	7.6	—	—	1	165	106.7
SEBS[g]	Shell	83,700	1.04	—	—	−49 83	—	—
SEBS-*g*-MA[h]	Shell	85,000	1.15	—	—	−47 79	—	—
SBS[i]	Shell	120,000	1.35	—	—	—	—	—

[a] For PP samples, GPC in 1,2,4-trichlorobenzene with PP standards. For block copolymers, GPC in chloroform with PS standards.
[b] Pentades of polypropylene as determined by ^{13}C-NMR in $C_2D_2Cl_4$ at 75.4 MHz, calibrated with solvent peak at 74.2 ppm.
[c] Determined by dynamic mechanical analysis in a Rheometrics solid analyzer.
[d] Determined with heating and cooling rates of 20°C/min in a Perkin–Elmer DSC7.
[e] Prepared in our laboratory.
[f] Shell KM6100®.
[g] SEBS: Kraton® G1652, 29 wt % styrene. The polybutadiene precursor of the olefinic block had 40% 1,2 and 60% 1,4 modes of enchainment.
[h] SEBS-*g*-MA: Kraton® FG1901x, 29 wt % styrene grafted with 1% MA.
[i] SBS: Cariflex® KX210, 29 wt % styrene, contains also diblock copolymer.

sible to form core shell particles with a rigid polyamide core and a soft elastomer shell for this system to improve the strength and toughness without sacrificing stiffness.[14] Furthermore, SAXS and WAXS measurements showed that SEBS reduces the crystallinity of PP in ternary blends with high impact PS.[15]

Far less is known about the morphology of the binary system SEBS with isotactic PP (*i*-PP) and nothing is known about blends of SEBS with syndiotactic PP (*s*-PP). The modulus and the yield stress decrease in blends of *i*-PP with SEBS when the block copolymer amount is increased.[16–19] Now it should be interesting to study the morphology of blends of SEBS with *s*-PP and *i*-PP, respectively, and to correlate the morphology with mechanical data. The reason for good compatibility between SEBS and PP might be the random copolymer character of the EB block. Formally the EB block can be considered as a random copolymer with ethene and but-1-ene segments. The repulsion effect[20] of the different segments (even though the repulsion between ethene segments and but-1-ene segments is very small) might contribute to improved miscibility with PP compared to the highly immiscible homopolymer pairs PE/PP and polybutylene/PP. A better quantitative understanding of the miscibility of polyolefin model copolymers can be achieved by a solubility parameter approach,[21–23] based on the concept of regular solutions. This approach is obviously superior compared to the random copolymer blend theory or a theory based on different segment length.[23] It has also been found experimentally that PP is miscible with copolymers equivalent to the EB block, only when the the content of the 1,2 enchainment is high. But blends of PP with SEBS must always remain heterogeneous because the PS block is highly incompatible with PP.

Therefore, blends of *i*-PP and *s*-PP, containing different amounts of SEBS or SEBS-*g*-MA, respectively, were prepared. The morphology was studied by means of scanning electron microscopy (SEM) and transmission electron microscopy (TEM). Furthermore, mechanical properties such as modulus, yield strength, and elongation at break were measured and discussed. Two-layer specimens of *i*-PP and SEBS (SEBS-*g*-MA) were prepared in order to study interfacial properties.

EXPERIMENTAL

Materials

All materials and some characteristic data are listed in Table I. The details of the PP synthesis are given in Table II.

Table II Details of PP Synthesis

Toluene as Solvent 2-I Batch Reactor					
Polymer	Catalyst	[Zr] (μmol/L)	[Al] (mmol/L)	Temperature (°C)	Pressure (bar)
i-PP108k	I	2	20	40	2
s-PP104k	II	20	50	20	2
Continuous Gas Phase Reactor					
Polymer	Catalyst	[Zr] (μmol/100 g)	[Al] (mmol/100 g)	Temperature (°C)	Pressure (bar)
i-PP183k	I	70	225	70	28

I,*rac*-dimethylsilylbis(2-methylbenz[e]indenyl)zirconium(IV)dichloride/MAO;II,*i*-propyl(cyclopentadienyl)(1-fluorenyl)zirconium(IV)-dichloride/MAO.

Blend Preparation for SEM and TEM Measurements

The PP blends containing 30 or 70 wt % SEBS were prepared as follows. PP (*i*-PP108k or *s*-PP104k) and SEBS were dissolved in boiling toluene for 15 min to form a clear solution (6 wt % total). This viscous solution was slowly poured into a 10-fold excess of methanol under vigorous stirring. After 1 h the polymer blends were isolated and dried in a vacuum oven at 80°C for 3 days. The powder was placed in a vacuum hot press. Test specimens were pressed for 10 min at 180°C and a pressure of 10 bar. These specimens were slowly cooled without pressure to room temperature within 1 h. The preparation of the two-layer specimens is described below.

Melt Blends for Mechanical Testing

The large difference in melt viscosities of the neat polymers makes it difficult to achieve a good mixing in a short time at relatively low temperatures. When the temperature or the shear is too high, PP degrades very fast. Therefore, 1000 ppm Irganox® 1010 in combination with 500 ppm Irganox® 656 and 500 ppm Irgafos® 168 (Ciba–Geigy AG) were added as stabilizers. The components (*i*-PP183k or *s*-PP106k with SEBS) were then premixed in a mill for 3 min to reduce the kneading time and temperature. The melt blends were prepared in a Haake Rheocord 90 batch mixer with contrarotating roller blades in a 70-cm^3 chamber operating at 175°C and 100 rpm. After 4 min of mixing the blends were quenched to room temperature. After annealing at 200°C for 30 min under vacuum in a hot press (Schwabenthan, Polystat 100), 2-mm thick disk specimens with 145-mm diameter were pressed for 5 min. Then the form was rapidly transferred into another water-cooled press.

Stress–Strain Measurements

For mechanical testing the plates were conditioned at room temperature and were cut and machined to obtain 18-mm tensile test specimens (DIN 53455). Stress–strain experiments to determine the modulus, yield strength, strain at yield, and elongation at break were performed with a crosshead speed of 10 mm/min on an Instron 4204. A minimum of five specimens was tested.

Notched Charpy Impact Strength

Notched specimens with dimensions of 60 × 13 × 2 mm with a notch depth of 3 mm but no crack initiation, were cut and tested using a Zwick model 5102 equipped with a 1, 2, or 4 J pendulum according to DIN 53453.

Peel Test

As described above for each polymer (*i*-PP46k and SEBS or SEBS-*g*-MA), plates of 2-mm thickness were pressed under vacuum at 240°C. Bars with the dimensions of 50 × 9 × 2 mm were cut out of the plates. Two-layer specimens were prepared by mounting the bars of each polymer together. A distance holder of 3.7 mm was used to prevent the block copolymer from deforming during the pressing. Silicone sheets above and below the specimen ensured a uniform pressure. The polymers were pressed on

each other for times between 30 min and 16 h at 165°C, and then rapidly cooled to room temperature. These specimens were partially separated at the interface using a razor blade. The SEBS layer was bent and fixed in the Instron machine. The force necessary to separate the two layers was measured. The average delamination force was normalized by the width of the specimen to calculate the peel strength (N/mm).

SEM

Two types of specimen preparations, cryofracture and etching, were used to get maximum contrast and picture quality. Cryofracture: The hot pressed specimens, 40 × 6 × 2 mm, were stored in liquid nitrogen for 5 min. Then they were broken just above the surface of the liquid nitrogen with maximum velocity. Etching: The same type of specimens were cut with a razor blade and then dipped into tetrahydrofuran (THF) for 5 min at room temperature. All samples were washed with acetone and dried in vacuum. Then they were sputtered with gold in a Scientific-Instruments minicoater (air 200 mbar, 20 mA, 2 min). A Zeiss DSM 960 scanning electron microscope was used in secondary electron mode at 10–20 kV.

TEM

TEM measurements were done with a Zeiss CEM 902 transmission electron microscope applying an acceleration voltage of 80 kV. The specimens were cut by an ultramicrotome (Ultracut E, Reichert & Jung, equipped with a diamond knife) at room temperature. The blends containing 70 wt % SEBS and the two-layer specimens were cryosectioned at −150°C. Ultrathin sections of approximately 70-nm thickness were stained with RuO_4 prepared from 100 mg $RuCl_3$ and 5 mL of 10 wt % NaClO solution over the gas phase.[24,25] After a staining time of 10 min in the RuO_4 gas phase, only the PS of the block copolymer was stained. If the staining time was extended to 2 h, the lamellae of the PP could also be distinguished.

RESULTS AND DISCUSSION

First the morphologies of the blends prepared by precipitation from a common solvent should be discussed because some of the mechanical properties are closely associated with the superstructure of immiscible polymer blends. Figure 1 shows SEM pictures of the cryofracture surface of blends of SEBS with *i*-PP108k (a,b) and with *s*-PP104k (c,d) prepared under exactly the same conditions as explained in the experimental part. In Figure 1(b) and (d) the SEBS phase is removed with THF at room temperature. Figures 1(a) and (c) show that the adhesion between the particles is good because single particles, removed during the fracture process, cannot be observed. The blends of *i*-PP108k with SEBS show a more interconnected phase morphology with relatively large spacings [Fig. 1(b)]. The SEBS particles in blends with *s*-PP104k are smaller and more separated from each other [Fig. 1(d)]. Generally, more information can be obtained from TEM measurements because of the higher resolution. Figure 2 depicts TEM micrographs of a mixture of *i*-PP108k/SEBS (70/30 wt %). In Figure 2(a), a clearly bimodal phase morphology can be distinguished. large irregularly formed particles of more than 1 μm coexist with spherical particles of an average diameter of approximately 150 nm. The block copolymer phase can be seen as dispersed particles. The microphase separation cannot be observed because of the low magnification. The interface of the very large particles failed partially during the microtoming. These holes appear to be dark because this micrograph was obtained in the electron energy loss mode. With the higher magnification of Figure 2(b), it can be seen that the interface between the block copolymer and *i*-PP108k initiates the crystallization of *i*-PP108k. Lamellae can clearly be seen at the interface but not in the bulk phase, indicating a nucleation effect. Finally, Figure 2(c) shows a part of the interface between a SEBS domain and the *i*-PP108k matrix. The block copolymer is clearly microphase separated and shows dark PS microdomains with a spacing of about 15–20 nm. The *i*-PP108k bulk phase contains the typical cross-hatched lamellae. The lamellae at the interface have a completely different appearance: they are thicker and grow mostly in a direction perpendicular to the interface. This is typical for transcrystallinity and is caused by the fact that the phase boundary acts as a nucleation agent. Transcrystallinity is usually observed by light microscopy that is not able to show the crystallization on a lamellar scale.[26–28] Figure 3(a) depicts an interface between the *i*-PP108k phase and the SEBS phase, which failed partially during microtoming. It can be seen that the interfacial failure did not occur at the interface itself, but between the first and second layer of PS microdomains in the SEBS phase. Thus it can be concluded that the interfacial adhesion between SEBS and *i*-PP108k is relatively strong. For blends of *s*-PP104k

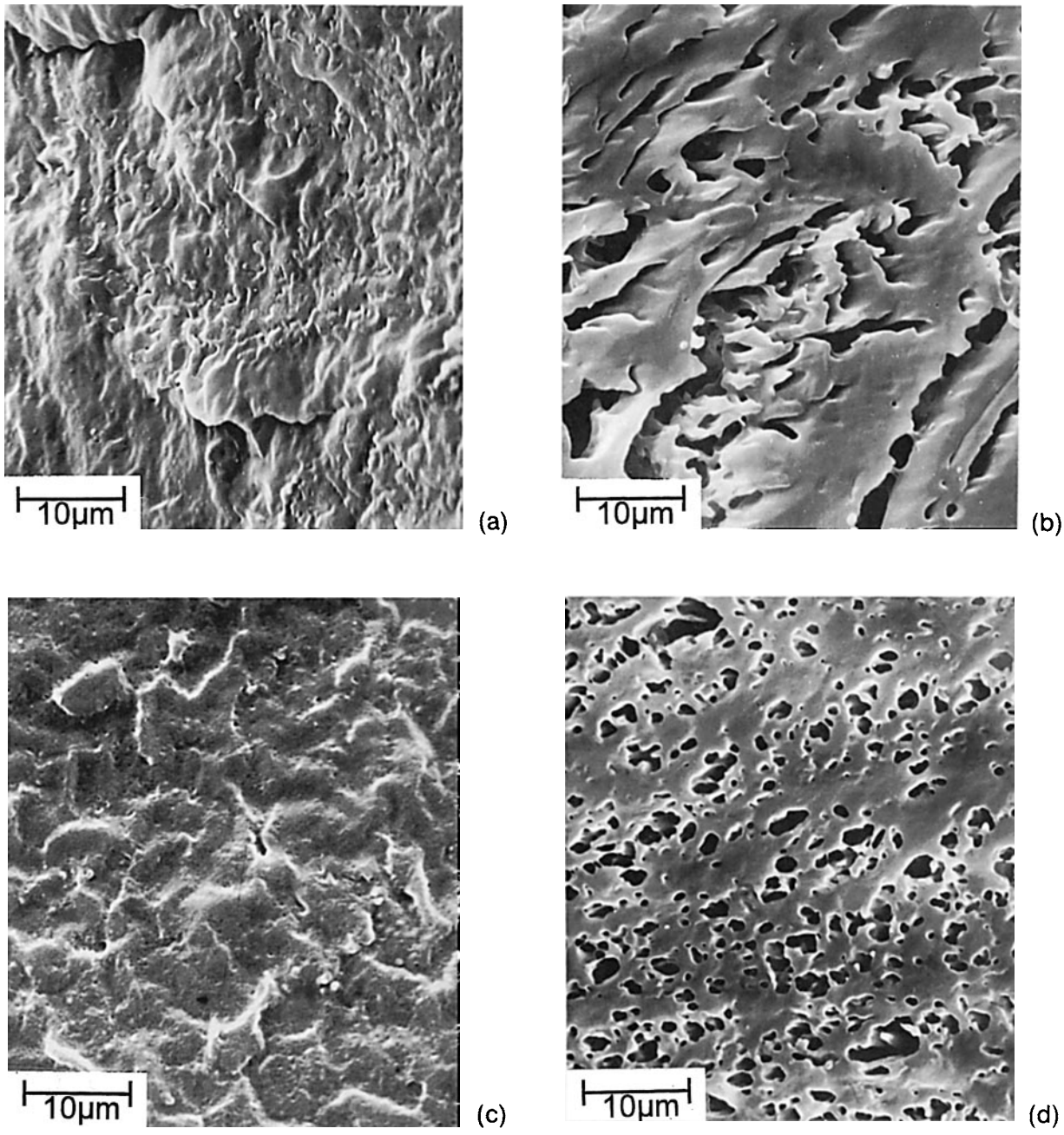

Figure 1 SEM micrographs of PP/SEBS blends (70/30 wt %). (a) Cryofracture surfaces of *i*-PP108k/SEBS, (b) *i*-PP108k/SEBS after SEBS was removed in THF, (c) cryofracture surfaces of *s*-PP104k/SEBS, and (d) *s*-PP104k/SEBS after SEBS was removed in THF.

with SEBS, the morphology observed by TEM was very similar to the blends of *i*-PP108k with SEBS; but because of its lower modulus, the microtoming was much more difficult. Single lamellae of crystallized *s*-PP104k were not observed. Figure 3(b) shows that in the case of *i*-PP108k/SEBS (30/70 wt %) blends, SEBS micelles are dispersed in the *i*-PP phase. These micelles are regularly formed and contain different numbers of PS microdomains. Figure 3(c) shows a three-dimensional image of the zoomed upper right part of Figure 3(b). Different types of micelles can be distinguished. The most simple type contains only one sphere of PS in the center surrounded by the EB blocks and PP. The surrounding EB block cannot be observed because a selective staining is impossible. Other micelles have different

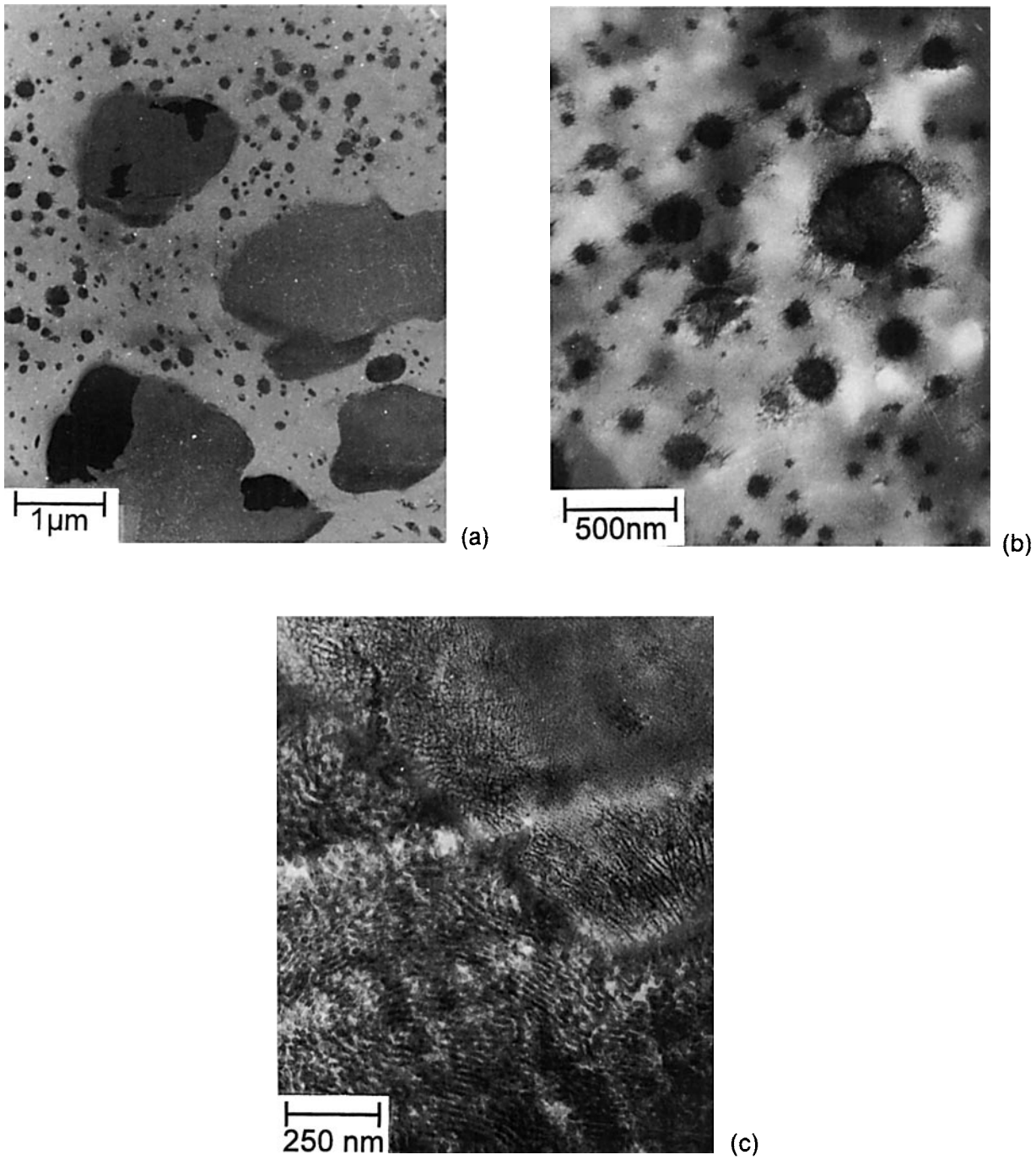

Figure 2 TEM micrographs of *i*-PP108k/SEBS (70/30 wt %) blends. (a) Bimodal particle size distribution of SEBS in *i*-PP108k, (b) growing *i*-PP108k lamellae at the *i*-PP108k/SEBS interface, and (c) microphase separated block copolymer structure and different crystalline regions of *i*-PP108k.

geometries. They contain one or more PS spheres in the center. They are surrounded in a certain distance by rings formed by several PS spheres. There is also one micelle that is formed only by a ring without a PS sphere in the center.

Now the interface between SEBS and PP should be studied in more detail. Figure 4(a) shows a TEM micrograph of a bilayer specimen annealed for 2 h at 165°C and microtomed perpendicular to the interface. It can be seen that the EB block must have

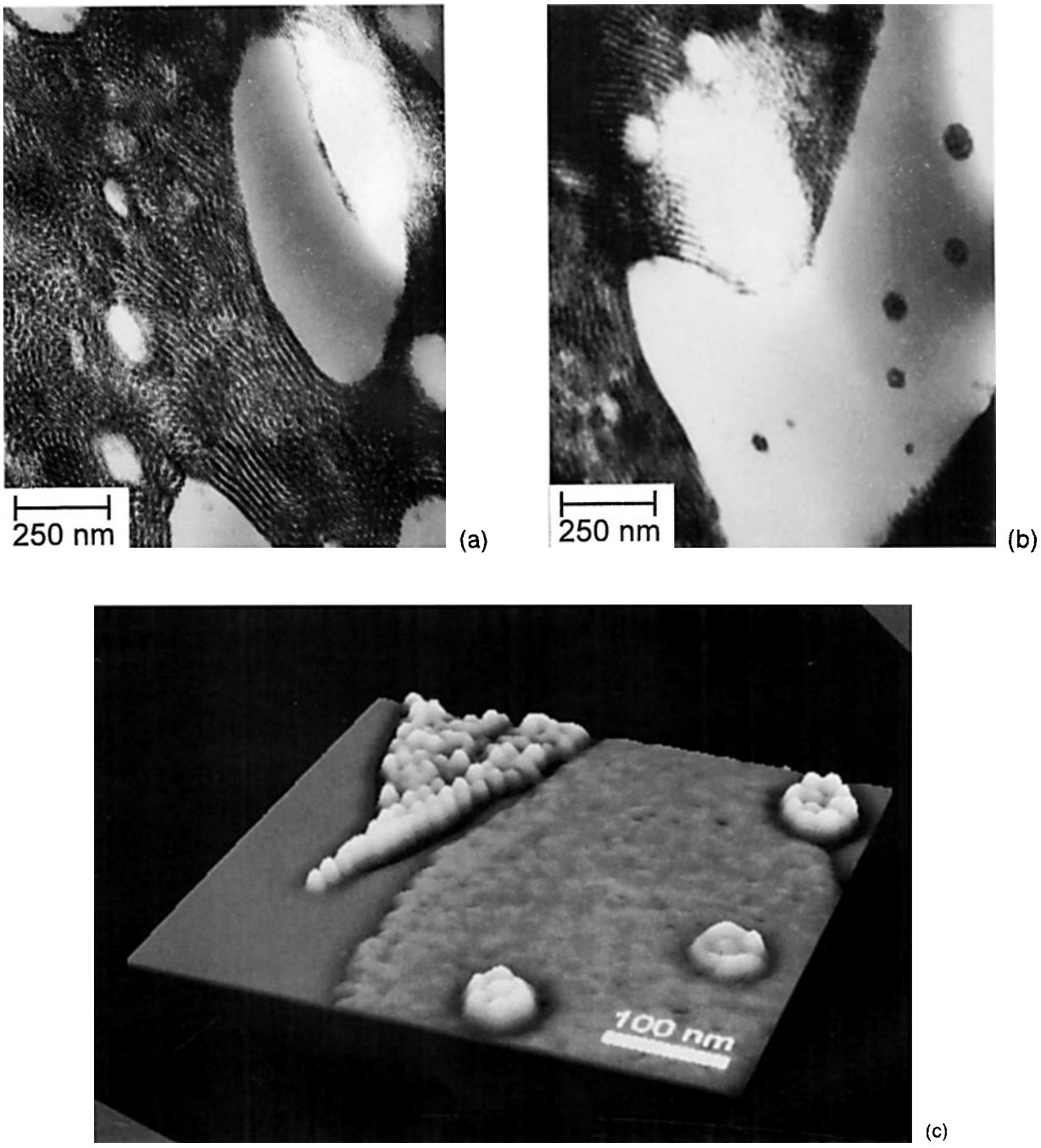

Figure 3 TEM micrographs of *i*-PP108k/SEBS (30/70 wt %) blends. (a) Failed interface between SEBS and *i*-PP108k, (b) SEBS micelles in an *i*-PP108k matrix, and (c) three-dimensional image of the upper right part of (b) obtained from the gray value distribution.

a good solubility in the *i*-PP46k phase, because the whole block copolymer tends to migrate into the polyolefin phase. As discussed in the Introduction, the EB block having this copolymer composition should be immiscible with PP.[23] But the tendency of the block copolymer to migrate into the *i*-PP phase is obvious. It can be assumed that a good solubility of the EB block in the *i*-PP46k phase is the driving force for this process. It must be taken into consideration that the *i*-PP46k used for these measurements has a relatively low molecular weight and a broad molecular weight distribution. Because the

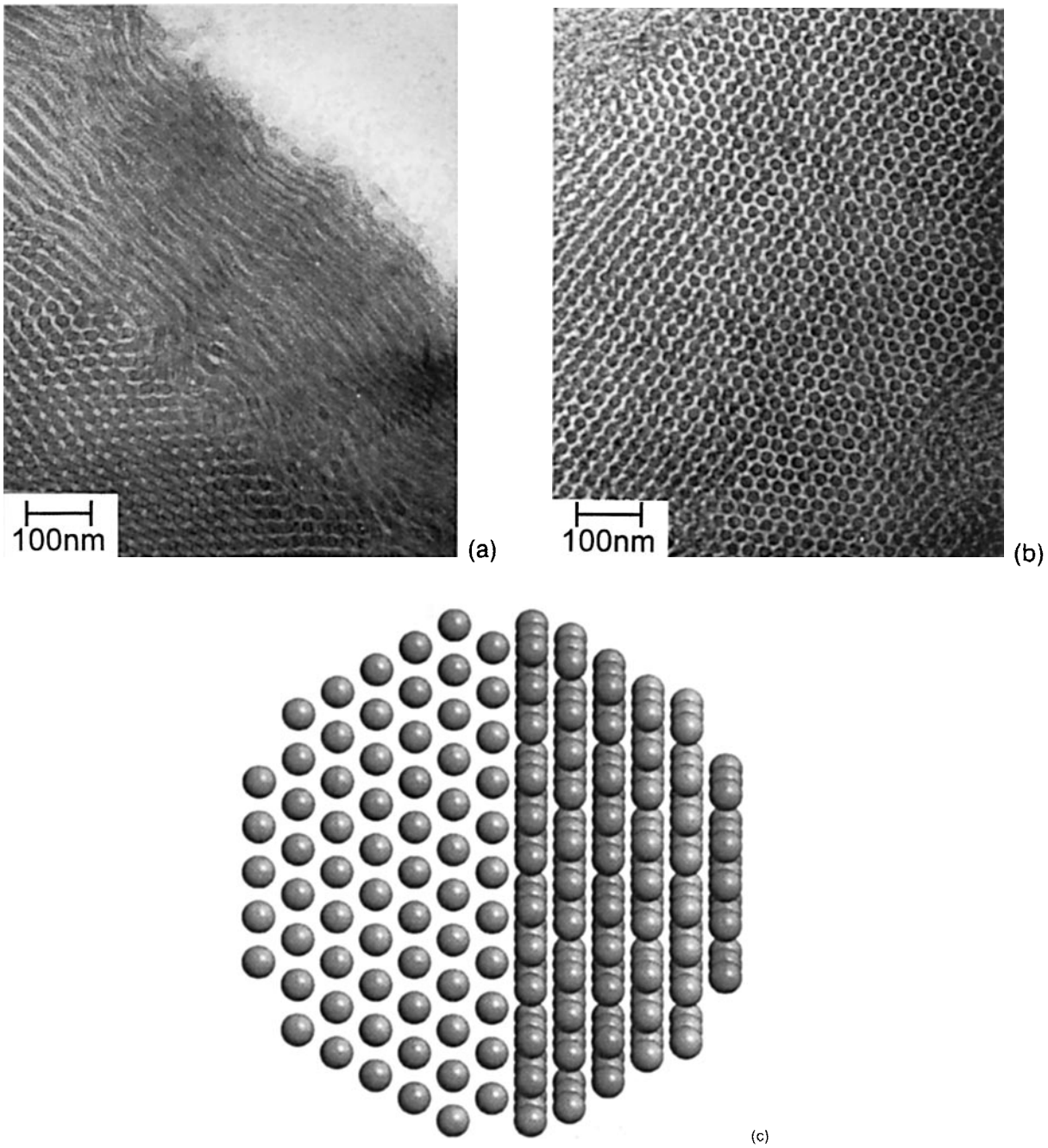

Figure 4 TEM micrographs taken after an annealing time of 2 h at 165°C. (a) Two-layer specimen of *i*-PP46k and SEBS microtomed perpendicular to the interface, (b) ultrathin section of the SEBS bulk phase, and (c) simulation of the TEM micrographs using Schakal® software.

enthalpic interactions in polyolefin blends are very small, entropic contributions and also small differences in chain tacticity might influence the miscibility behavior significantly. The block copolymer micelles can be seen as darker areas in the *i*-PP46k phase, but the *i*-PP46k is also able to swell the outermost parts of the SEBS phase. This might contribute to an apparently lamellar arrangement of PS domains parallel to the interface. For neat SEBS, different types of the arrangement of the microphases have been reported.[29,30] Lamellae, cylindrical, or spherical microphases were formed during the

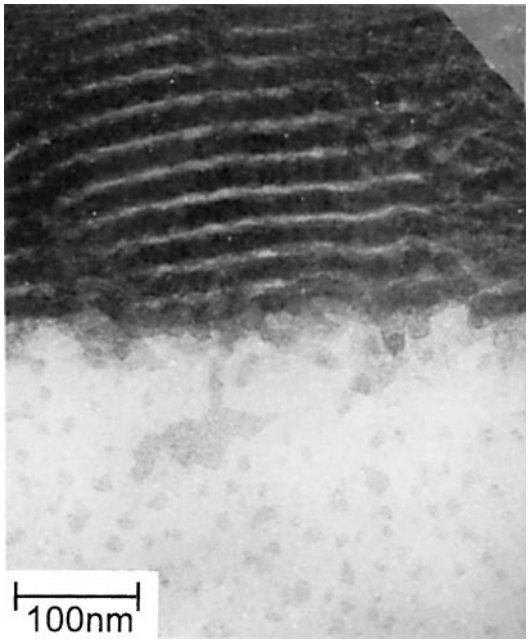

Figure 5 (a) TEM micrograph of the interface between SEBS and *i*-PP46k after an annealing time of 2 h at 165°C and (b) Three-dimensional image of (a) obtained from the gray value distribution.

evaporation of different solvents. Our TEM measurements of samples isothermally annealed in the melt did not show any lamellae or cylindrical structures [see Fig. 4(b)]. Thus it can be assumed that spherical microdomains are formed that should be arranged in a body centered cubic (bcc) lattice.[31,33] The spheres in Figure 4(b) have an apparently hexagonal arrangement. But Figure 4(c) shows that the TEM micrographs of Figure 4(a) and (b) can be explained with a bcc lattice. For the simulations, a section with the thickness of three diameters of the spheres were used. This is also the approximate thickness of the ultrathin sections for TEM. The left part shows the (111) projection of the bcc lattice. This leads to the picture of spheres with the six next neighbors as seen in Figure 4(b), but the bcc lattice has eight next neighbor. That means, two of them cannot be seen because they are exactly on top and below the center sphere. Also the apparently lamellar microdomains at the interface can be explained. The right part of Figure 4(c) also shows the bcc lattice, but tilted by an angle of 15°. This shows clearly that the apparent lamellae at the interface, as shown in Figure 4(a), are composed of single spheres. Thus it seems possible that before the dissolution process starts at the interface, a stress acts on the microdomains that results in a cooperative tilting process.

Figure 5(a) and (b) show the dissolution process of the block copolymer at the interface in more detail. The migration of microdomains starts at the interface between the block copolymer and *i*-PP46k. Obviously the roughness of the outermost layers of the block copolymer increases and then single PS microdomains start to separate from the block copolymer and move toward the bulk of the *i*-PP46k

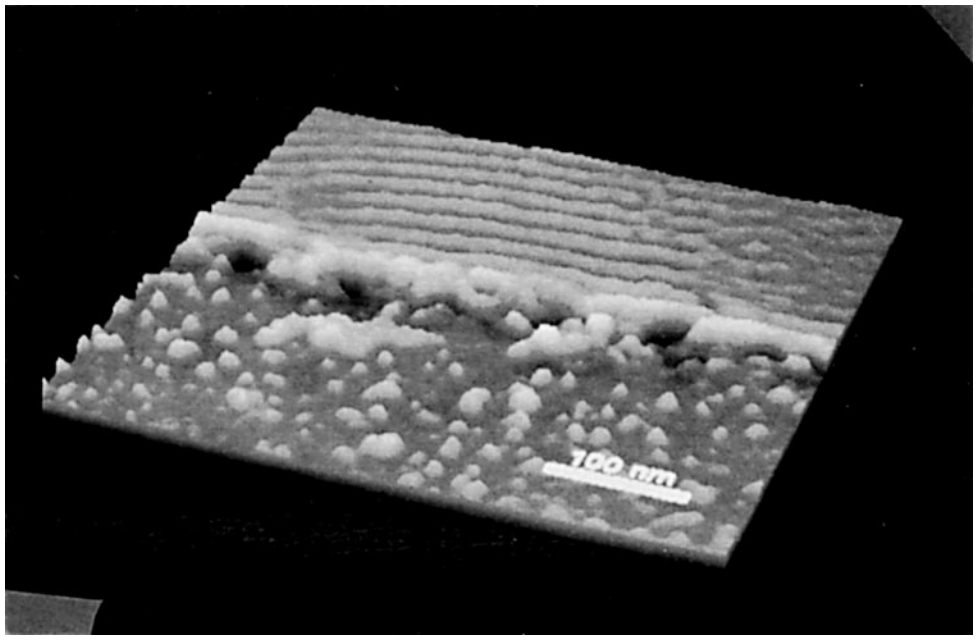

Figure 5 (*Continued*)

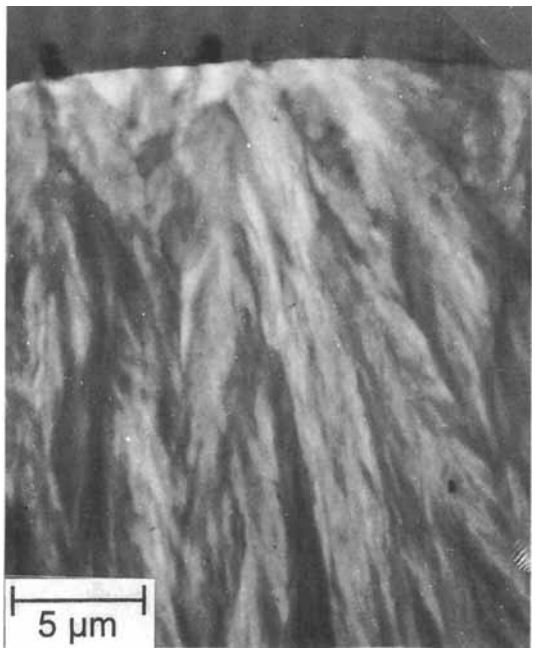

Figure 6 Same sample as in Figures 4 and 5 but lower magnification. Fibrills of the transcrystalline regions of *i*-PP46k can be seen.

phase. In the beginning these PS microdomains have a sharp contour. During the migration away from the interface the microdomains dissolve and form micelles. They diffuse deeper into the *i*-PP46k phase and simultaneously the size of the micelles decreases.

Figure 6 shows a TEM micrograph of the crystalline region of *i*-PP46k near the interface with SEBS. The sample is the same as discussed in Figures 4 and 5. Because of the low magnification the SEBS microstructure cannot be observed, but the formation of transcrystals of *i*-PP46k can be seen. Transcrystals are found because the interface may act as a nucleation agent for *i*-PP,[34] as already discussed above. The high nucleation density does not allow the formation of spherulites but forces the lamellae to grow perpendicular to the interface. On the micrograph only fibrils can be observed that are composed of several lamellae.

On the basis of insight into morphological features, it is now possible to understand the mechanical properties. Figure 7 depicts three typical results of a peel test obtained from two-layer specimens after different annealing times. The plateau of the delamination force divided by the width of the specimen is defined as the peel strength. The plateau value of the delamination force was calculated by everaging the force values between 30 and 90% of the crosshead distance. It should be mentioned that

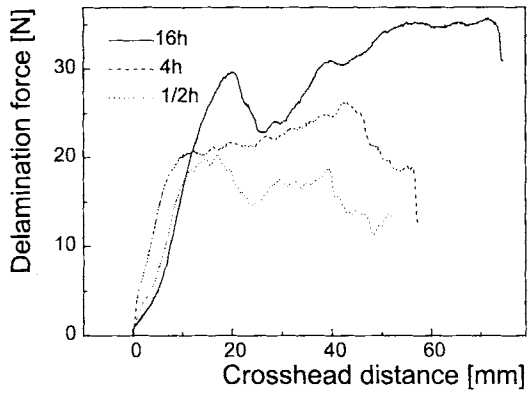

Figure 7 Crosshead distance versus delamination force of the peel test of two-layer specimens of *i*-PP46k and SEBS after different annealing times.

the SEBS also deformed during the test. Thus the peel strength reflects the reality, but the delamination work is altered by the strain of the SEBS. The measured peel strength as a function of annealing time can be seen in Figure 8. The test was carried out for two different SEBS types; one of them was maleinated. It can be seen that in both cases the peel strength increases with annealing time and reaches a plateau. The increase is in agreement with the TEM micrographs. The interdiffusion between the EB blocks of SEBS and PP increases the interfacial thickness and thus the number of chains crossing the interface. But the increase is limited by the fact that after a certain time the block copolymer migrates completely into the PP phase and forms micelles. Furthermore, it is evident that the SEBS-*g*-MA leads to a lower peel strength. This is obviously caused by the stronger repulsion of the very polar succinic anhydride groups of the maleinated

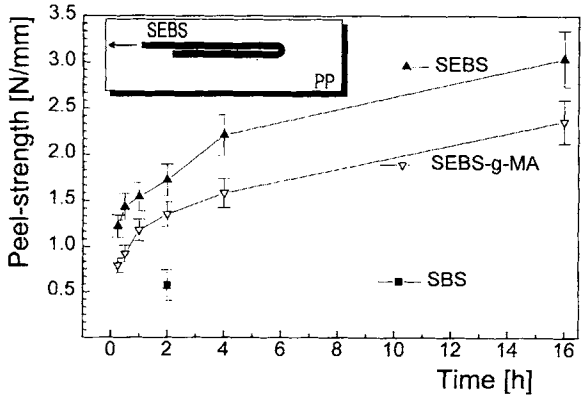

Figure 8 Peel strength versus annealing time at 165°C for two-layer specimens of *i*-PP46k with SEBS or with maleinated SEBS. The inset shows the sample geometry.

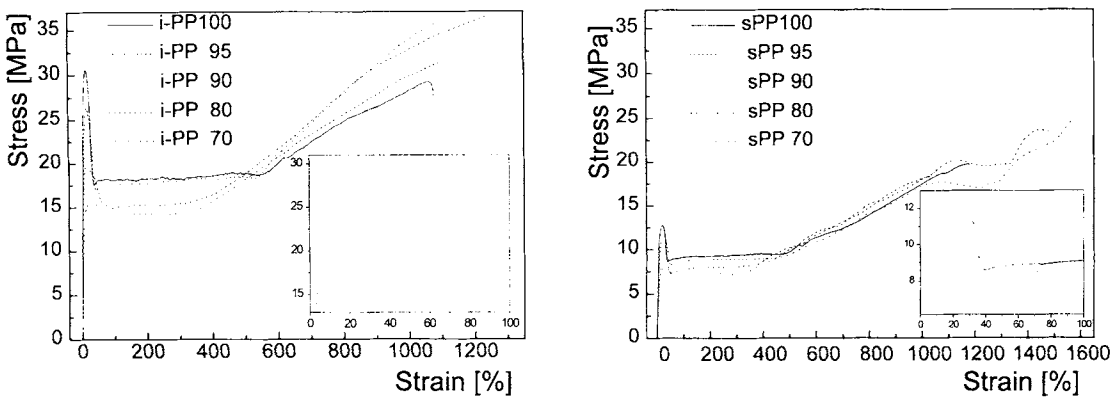

Figure 9 Stress–strain curves of blends of (a) *i*-PP183k/SEBS and (b) *s*-PP106k/SEBS. The inset shows the yield maximum enlarged.

SEBS with the very unpolar *i*-PP. These measurements were carried out 12 h after the thermal annealing. This has to be taken into consideration because aging phenomena may change the mechanical properties. A two-layer specimen of a triblock copolymer of poly(styrene)-*block*-poly(butadiene)-*block*-poly(styrene) (SBS) with *i*-PP46k had, after the annealing time of 2 h at 165°C and storing for 12 h, a peel strength of only 0.57 N/mm that reflects a high degree of incompatibility.

Finally, Figure 9(a) and (b) show stress–strain curves for blends of SEBS with *i*-PP183k and *s*-PP106k, respectively. The insets show the yield areas enlarged. Our measurements show that the addition of SEBS to *i*-PP183k as well as to *s*-PP106k decreases the yield strength, the modulus, and the flow plateau. The yield maximum becomes broader and elongation at break becomes higher with increasing content of the thermoplastic elastomer. All the specimens showed well-defined necking after reaching the yield maximum. During the flow plateau after the yield point, the necking region expands over the deformation zone. Thus the tensile stress keeps almost constant with increasing strain. After the necking is completed, the tensile stress increases again monotonically with strain. With an increasing amount of SEBS in the blends, the necking starts later and ends earlier. Pure SEBS does not show any yield maximum and consistently necking does not occur.

Adding SEBS leads to an improvement of the impact strength of *i*-PP and also *s*-PP. For *i*-PP blends with SEBS, the same result was obtained by Gupta and Purwar.[35] The addition of 10 wt % SEBS to *i*-PP makes the measurement of Charpy impact strength impossible because the specimens do not break after impact. It can be seen that the impact energy is dissipated into a large area of the material. This was reflected by a strain induced birefringence. Also neat *s*-PP106k does not fail without adding SEBS.

CONCLUSION

It has been shown that SEBS has a good interfacial adhesion with *i*-PP and *s*-PP surfaces. SEBS tends to diffuse into *i*-PP as well as into *s*-PP under micelle formation. This might be a disadvantage when SEBS is also used as a compatibilization agent in ternary blends, because SEBS is expected to be located at the interface. Using maleinated SEBS instead of SEBS decreases the peel strength between the block copolymer and *i*-PP. Adding SEBS to *i*-PP and *s*-PP decreases the modulus, the yield strength, and the flow plateau. It improves the impact strength and the elongation at break.

This AIF project Nr. 8529 was financially supported by the Bundesminister für Wirtschaft. Dr. W. Heckmann, BASF, carried out the cryomicrotoming. S. Jüngling provided *i*-PP108k and *s*-PP104k samples. The commercial grade of *s*-PP106k was supplied by Mitsui Toatsu. The *i*-PP46k sample and the SEBS samples were supplied by Shell.

REFERENCES

1. G. Holden and N. R. Legge, in *Thermoplastic Elastomers*, N. R. Legge, G. Holden, and H. E. Schroeder, Eds., Hanser Pub., Munich, 1987.
2. G. H. Michler, *Kunststoff Mikromechanik: Morphologie, Deformations- und Bruchmechanismen*, Hanser Pub., Munich, 1992.
3. R. Fayt, R. Jerome, and Ph. Teyssie, *J. Polym. Sci., Polym. Phys.*, **27**, 775 (1989).

4. R. Fayt, R. Jerome, and Ph. Teyssie, *Polym. Eng. Sci.*, **27,** 328 (1987).
5. C. Creton, E. J. Kramer, C. Y. Hui, and H. R. Brown, *Macromolecules,* **25,** 3075 (1992).
6. K. R. Srinivasan and A. K. Gupta, *J. Appl. Polym. Sci.*, **53,** 1 (1994).
7. A. K. Gupta and K. R. Srinivasan, *J. Appl. Polym. Sci.*, **47,** 167 (1993).
8. M. Frounchi and R. P. Burford, *Iranian J. Polym. Sci. Technol.*, **2,** 59 (1993).
9. A. K. Gupta and S. N. Purwar, *J. Appl. Polym. Sci.*, **30,** 1799 (1985).
10. M. C. Schwarz, J. W. Barlow, and D. R. Paul, *J. Appl. Polym. Sci.*, **37,** 403 (1989).
11. J. Rösch, T. Duschek, and R. Mülhaupt, *Polym. Adv. Technol.*, **4,** 465 (1993).
12. M. Holsten-Miettinen, J. V. Seppälä, O. T. Ikkalla, and I. T. Reima, *Polym. Eng. Sci.*, **34,** 395 (1994).
13. J. Modic and I. A. Pottick, *Polym. Eng. Sci.*, **33,** 819 (1993).
14. J. Rösch and R. Mülhaupt, *Polym. Bull.*, **32,** 697 (1994).
15. D. Hlavata and Z. Horak, *Eur. Polym. J.*, **30,** 597 (1994).
16. A. K. Gupta and S. N. Purwar, *J. Appl. Polym. Sci.*, **30,** 1777 (1985).
17. A. K. Gupta and S. N. Purwar, *J. Appl. Polym. Sci.*, **29,** 3513 (1984).
18. A. K. Gupta and S. N. Purwar, *J. Appl. Polym. Sci.*, **29,** 1592 (1984).
19. A. K. Gupta and S. N. Purwar, *J. Appl. Polym. Sci.*, **29,** 1079 (1984).
20. G. ten Brinke, F. E. Karasz, and W. J. MacKnight, *Macromolecules,* **16,** 1827 (1983).
21. D. J. Walsh, W. W. Graessley, S. Datta, D. J. Lohse, and L. J. Fetters, *Macromolecules,* **25,** 5236 (1992).
22. R. Krishnamoorti, W. W. Graessley, N. P. Balsara, and D. J. Lohse, *Macromolecules,* **27,** 3073 (1994).
23. W. W. Graessley, R. Krishnamoorti, G. C. Reichhart, N. P. Balsara, L. J. Fetters, and D. J. Lohse, *Macromolecules,* **28,** 1260 (1995).
24. W. Heckmann, *Proc. Int. Congr. Electron Microsc., XIIth,* **4,** 854 (1990).
25. L. C. Sawyer and D. T. Grubb, *Polymer Microscopy,* Chapman & Hall, London, 1982.
26. H. Janneschitz-Kriegel, *Progr. Colloid Polym. Sci.*, **87,** 117 (1992).
27. N. Billon, C. Magnet, J. M. Haudin, and D. Lefebvre, *Colloid Polym. Sci.*, **272,** 633 (1994).
28. S. Setz, R. Schnell, R. Thomann, J. Kressler, and R. Mülhaupt, *Makromol. Rapid Commun.*, **16,** 81 (1995).
29. M. Kakugo, H. Sadatoshi, M. Yokoyama, and K. Kojima, *Polym. Commun.*, **29,** 288 (1988).
30. G. Cho and A. Natansohn, *Can. J. Chem.*, **72,** 2255 (1994).
31. F. S. Bates, *Science,* **251,** 898 (1991).
32. M. W. Matsen and M. Schick, *Macromolecules,* **27,** 7157 (1994).
33. E. L. Thomas, D. J. Kinning, D. B. Alward, and C. S. Henkee, *Macromolecules,* **20,** 2934 (1987).
34. F. L. Binsbergen, *J. Polym. Sci., Phys Ed.*, **11,** 117 (1973).
35. A. K. Gupta and S. N. Purwar, *J. Appl. Polym. Sci.*, **31,** 535 (1986).

Received April 4, 1995
Accepted July 29, 1995